[15] *Subroutine "ZXSSQ," IMSL Reference Manual,* 9th ed., Int. Mathematical and Statistical Libraries, Inc., June 1982.
[16] C. Rauscher, "Large-signal technique for designing single-frequency and voltage-controlled GaAs FET oscillators," *IEEE Trans. Microwave Theory Tech.*, vol. MTT-29, pp. 293–304, Apr. 1981.

Christen Rauscher (S'73–M'75–SM'81) was born in Boston, MA, on November 4, 1944. He received the diploma in electrical engineering and the Ph.D. degree in 1969 and 1975, respectively, both from the Swiss Federal Institute of Technology, Zurich, Switzerland.

From 1969 to 1976 he was employed as an Assistant and Research Associate at the Microwave Laboratory of the Swiss Federal Institute of Technology where he conducted research on computer-aided tolerance optimization of microwave active circuits and on IMPATT power amplifiers. He held a Postdoctoral Fellowship from the Swiss National Science foundation from 1976 to 1978. He spent this time at Cornell University, Ithaca, NY and the Naval Research Laboratory, Washington, DC, investigating the nonlinear behavior of GaAs MESFET's. Since 1978 he has been employed at the Naval Research Laboratory, Washington, DC, engaged in research on microwave and millimeter-wave nonlinear circuits.

Design and Analysis of the Channel Waveguide Transformer

PETER H. SIEGEL, STUDENT MEMBER, IEEE, DORN W. PETERSON, MEMBER, IEEE, AND ANTHONY R. KERR, SENIOR MEMBER, IEEE

Abstract—**The authors describe an easily fabricated *H*-plane transformer for use in rectangular waveguide carrying the dominant mode. An approximate theoretical analysis of the structure is presented, and computed results are compared with measurements on transformers at *X*-band. Design curves are given for transitions from full to one-half, one-third, and one-quarter height waveguide. The new transformers have been found particularly useful for millimeter-wave mixers and multipliers employing split-block construction. The structure can also be used as a transition from rectangular to channel waveguide.**

I. Introduction

WAVEGUIDE MIXERS and frequency multipliers often use reduced height waveguide for improved impedance matching to the nonlinear element. A stepped or tapered transformer is generally employed between the full and reduced height sections to minimize the mismatch. These transformers are especially difficult to fabricate at millimeter wavelengths where the guide dimensions are very small. Copper electroforming has been used successfully; however this process is time-consuming and usually requires the production of a disposable mandrel for each finished piece.

This paper describes a new form of *H*-plane transformer, particularly suitable for use in split-block rectangular waveguide, which can be made quickly and easily with a slitting saw or single-point cutting tool. The transformer has been used successfully in frequency doublers up to 220 GHz, and in mixers operating at 115 GHz.

A physical description of the transformer and detailed fabrication procedures are given in Section II. Section III outlines an approximate theoretical analysis for the determination of the reflection coefficient. The accuracy of the analysis is considered in Section IV where VSWR measurements of three *X*-band transformers are compared with computed values. In Section V, the theory is applied to two transformer configurations and design curves are given for transitions from full to one-half, one-third, and one-quarter height waveguide. Finally, in Section VI, two modifications are described which increase the bandwidth of the transformer.

II. Description of the Transformer

The channel waveguide transformer is shown in Fig. 1. It is most easily fabricated as a split-block structure in which the two halves are joined along a plane of zero transverse current (Fig. 1(d)). A slitting saw or single-point tool is used to cut the reduced height waveguide completely along the two blocks (Fig. 1(a)). The full height waveguide and transition region are then formed by moving the saw to each side of the centerline, producing a sloping channel in part of the block (Fig. 1(b) and (c)). The result is a length

Manuscript received November 2, 1982; revised February 7, 1983.
P. H. Siegel is with the Department of Electrical Engineering, Columbia University, New York, NY 10027.
D. W. Peterson is with the Department of Astronomy, Columbia University, New York, NY 10027.
A. R. Kerr is with the NASA/Goddard Institute for Space Studies, New York, NY 10025.

0018-9480/83/0600-0473$01.00 ©1983 IEEE

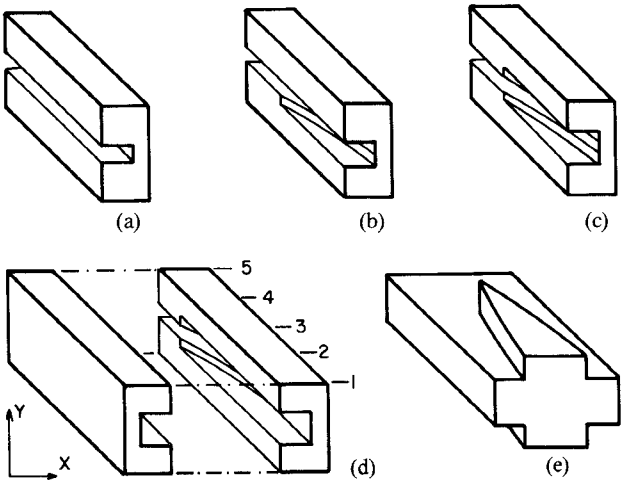

Fig. 1. (a) View of the right half of the transformer after machining the reduced height waveguide. (b) View of the right half of the transformer after the slitting saw has been used to produce one side of the transition from full to reduced height. (c) The complete right half. (d) An exploded view of the finished transformer. (e) A solid view of the transition region beginning about midway down the length of the taper.

of full height waveguide with sections of its narrow walls tapering in a circular arc towards the center until only the desired reduced height waveguide remains (Fig. 1(e)). Fig. 2(a) shows a series of cross sections along the longitudinal axis of the transformer, corresponding to the numbered positions in Fig. 1(d). The length of the taper is determined by the radius R of the slitting saw and the depth of cut (waveguide half-width) a according to $L = (2aR - a^2)^{1/2}$.

A taper with a linear rather than circular-arc-shaped profile can be formed by tilting the workpiece and moving it longitudinally under the slitting saw while the transition is being machined.

In cross section, the device resembles a symmetrical form of the channel waveguide described by Vilmur and Ishii [1]. An equivalent structure has also been termed cross-shaped [2] and crossed [3], [4] rectangular waveguide in the literature. The authors chose to use the term *channel waveguide* as it contrasts well with the more familiar ridged guide; one can think of the ridge as having been inverted to form a channel along the axis of propagation.

III. Theory and Analysis

A. The Characteristic Impedance Method

An approximate analysis of a taper of arbitrary cross section between two uniform waveguides propagating a single mode has been given by Johnson [5]. The tapered region is replaced by a series of short butt-jointed uniform waveguides each having its own propagation constant and guide impedance. Letting the number of sections become large and neglecting higher order modes and multiple reflections, Johnson arrived at the following expression for the reflection coefficient of the dominant mode:

$$\Gamma|_{z=0} = \frac{1}{2}\int_0^L \frac{d(\ln Z_c)}{dz} \exp\left[-2\int_0^z \gamma(z')\,dz'\right] dz \quad (1)$$

where the integration is over the length L of the transformer. For a gradual transition, $Z_c(z)$ can be equated with the characteristic impedance of a uniform waveguide having the same cross-sectional dimensions as the transformer at position z. $\gamma(z) = \alpha(z) + j\beta(z)$ is the propagation constant of the mode in each short section of guide and reduces simply to $j\beta(z)$ for a lossless transition. $\beta(z)$ is related to the cutoff wavenumber, $k_c(z)$ via

$$\beta = \left(\omega^2\mu\epsilon - k_c^2\right)^{1/2}$$

where $\omega = 2\pi f$ is the radian frequency of the incident wave and μ and ϵ are the permeability and permittivity of the medium in the transition. Considering each cross section in Fig. 2(a) to be that of a uniform waveguide, the value of the cutoff wavenumber $k_c(z)$ and hence the propagation phase constant $\beta(z)$ can be determined using the method of transverse resonance (see Appendix A). Approximate expressions for the transverse fields in the cross section can then be used to derive a waveguide characteristic impedance.

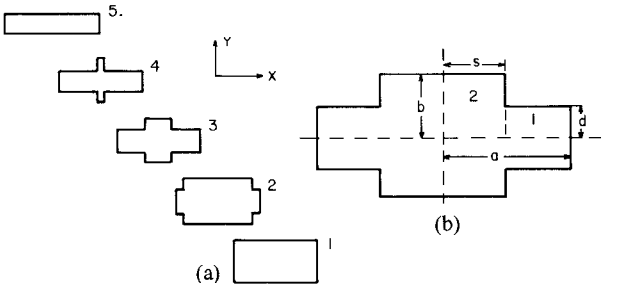

Fig. 2. (a) A series of cross sections taken along the length of the transformer. The numbers correspond to the positions indicated in Fig. 1(d). (b) A typical cross section defining the variables used in the theoretical analysis.

A second, though more laborious means of calculating k_c and Z_c along the length of the transition is to solve the wave equation in each section of uniform waveguide subject to the appropriate boundary conditions. Such an analysis was performed on the channel waveguide by Kuz'min and Makarov [2] and later by Tham [3] and Lin [4]. By breaking the cross section into two regions, expanding the fields in each region in a series of orthogonal functions, and matching the solutions across the boundary line, a matrix eigenvalue problem is set up. The lowest order eigenvalue is the wavenumber for the dominant mode in the guide, and the corresponding eigenvector contains the coefficients in the series expansion of the field. The fields can be integrated to determine the equivalent voltage and current used in calculating the characteristic impedance. The relevant equations are given in Appendix B, where a comparison is made between the different methods of calculating k_c and Z_c.

Once the values of $k_c(z)$ and $Z_c(z, f)$ have been determined, (1) can be integrated numerically to find Γ at a particular frequency.

The concept of a characteristic impedance for waveguides propagating a single mode is discussed by Shelkunoff [6]. For certain special cases, such as rectangular waveguide, there are three equally useful definitions which

differ only by constant factors. However, for non-TEM waveguides generally, and specifically for the channel waveguide structure, there is no obvious choice of expression for the characteristic impedance. The equivalent circuit of a junction between two waveguides with different cross sections can be described by a transformer, which couples between the wave impedances of the propagating mode in the two guides, and a shunt susceptance. To analyze the tapered channel waveguide rigorously by the characteristic impedance method, it is necessary to find a definition which results in a unity transformer ratio at each incremental change of cross section (as would be the case for a TEM or rectangular TE_{10}-waveguide taper using the conventional characteristic impedance definitions). Cohn [7] used a particular definition of characteristic impedance in analyzing ridged waveguide. As shown in Section IV, we have found that an analogous definition for channel waveguide gives acceptable agreement with experiment. However, we know of no way to prove that this definition actually does result in a unity transformer ratio.

B. The Method of Mode Coupling

The method of mode coupling[1] is a more general approach to the analysis of waveguides with slowly varying tapers. Early work by Schelkunoff [8] on a system of generalized Telegraphist's equations, and subsequent applications by Reiter [9], Solymar [10], and Katzenelenbaum [11] resulted in a general theory of coupled wave equations. This theory avoids using the concept of a characteristic guide impedance, and is not restricted to single-mode propagation. It was shown by Solymar [10] that the reflection coefficient of the dominant mode of a sufficiently gradual taper depends only upon the variation of two quantities along the taper: the wave impedance, and one of a set of mode coupling coefficients. The appropriate coupling coefficient, which describes coupling from the forward-traveling wave into the backward-traveling wave, is calculated from the transverse electric or magnetic field at each cross section of the transformer.

Since analytic expressions for the fields were available from [3] or [4], a concerted effort was made by us to apply Solymar's theory to the channel waveguide transformer. However, we found that it was not practical to predict the transformer performance with reasonable accuracy using this method. The problem appears to be the slow convergence of the series representing the fields in the channel waveguide.

Both the mode matching method of [3] and the Ritz-Galerkin method of [2] and [4] express the fields in the waveguide as infinite series satisfying the boundary conditions at each cross section. In any practical computation these series must be truncated. It was found that the matrix eigenvector problem could not be solved accurately unless the matrix was truncated at 5×5 or fewer elements. It is clear from Fig. 3 that the resulting electric field expressions

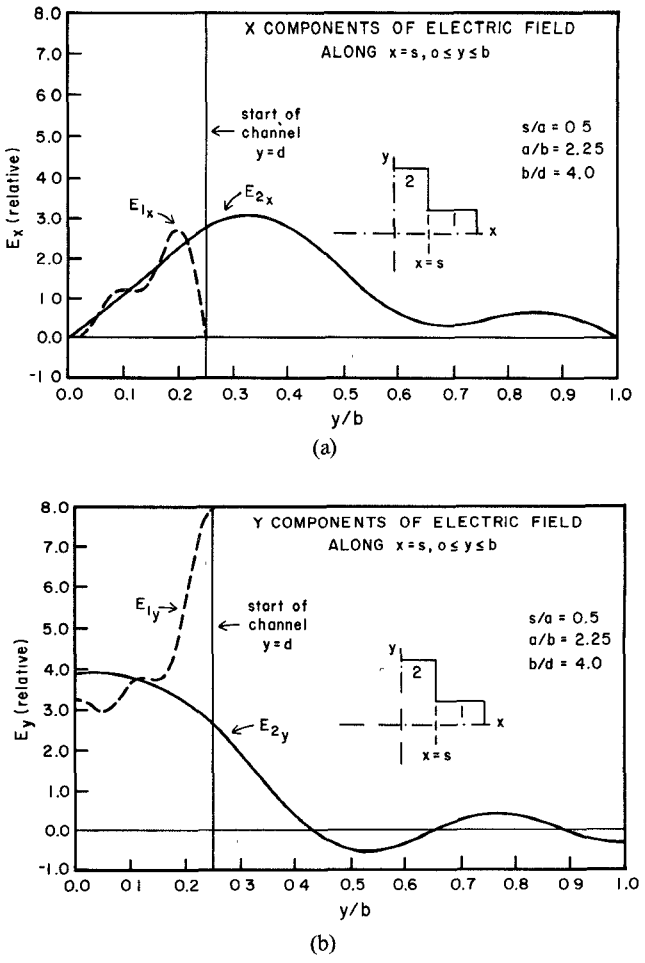

Fig. 3. (a) A plot of the x component of the electric fields along $x = s$, from $y = 0$ to $y = b$ when $s/a = 0.5$. This includes the boundary line at which the fields in the two regions of the cross section (see Fig. 2) are matched, and the side wall of the channel. The plot has been made using the field expansions given in Appendix B, with the series truncated to five terms. Ideally E_{2_x} should become infinite as y approaches d. (b) A similar plot of the y component of the electric fields. E_{1_y} and E_{2_y} should be equal from $y = 0$ to d and should become infinite as y approaches d. E_{2_y} must become zero when $y > d$.

are a poor approximation to the full series solution near the start of the channel, and especially in the region of the singularity at the obtuse corner. Montgomery [12] made the same observations when he used the Ritz-Galerkin method to find the fields of the ridged waveguide. It so happens that the backward wave coupling coefficient for the dominant mode of the channel waveguide is governed only by the fields along the side wall of the channel ($x = s$), where they are most poorly represented by the truncated series. One might expect that the value of the coupling coefficient as determined from this series would be too small. Indeed, it was found that one could get the mode coupling theory to agree with measured values of reflection coefficient if the coupling coefficient, as calculated from the truncated series expansions, was increased from two to four times.

An alternative approach to the mode coupling method would be to use a numerical finite difference scheme to determine the fields in the channel waveguide transformer more accurately, and then to use the small coupling theory

[1]A useful discussion of the method of mode coupling is given in the monograph by Sporleder and Unger [18].

of Solymar to calculate the reflection coefficient. Such an approach was used by Saad, Davies, and Davies [13] in the design of a Marie mode transformer.

C. Choice of Method

For the reasons described in the previous section, the characteristic impedance method was used in deriving the theoretical results given in this paper.[2]

The following steps summarize the algorithm used for determining the reflection coefficient of the channel waveguide transformer.

a) The input and output waveguide sizes are specified, together with expressions for the cross-sectional dimensions at any point along the length of the transition.

b) The transcendental equation in Appendix A, or the eigenvalue equation in Appendix B, is solved at each of a series of cross sections along the length of the transformer. The lowest order roots from either method yield the TE_{10}-mode cutoff wavenumbers $k_c(z)$. For the results presented in this paper, the transverse resonance method was used, as it requires much less computing time than the solution of the eigenvalue problem.

c) The waveguide characteristic impedance $Z_c(z)$ is obtained using either the transverse resonance method (Appendix A) or the eigenvalue method (Appendix B). Again, in this paper the transverse resonance method was used because of the saving in computer time.

d) The propagation phase constant $\beta(z)$ is found from the wavenumber, and the logarithmic derivative of the characteristic impedance is determined at each cross section along the length of the transformer.

e) The reflection coefficient Γ at the start of the taper is calculated from (1) by numerical integration.

f) Steps d) and e) are repeated at each frequency of interest.

IV. Comparison with Experiment

To check the accuracy of the analysis, three channel waveguide transformers having input to output height ratios of 2, 3, and 4 were fabricated in X-band waveguide (8.2–12.4 GHz). The transitions used linear tapers with half angles of 8 and 10 degrees, and lengths approximately one guide wavelength (as measured in X-band rectangular waveguide) at 8 GHz. The voltage standing wave ratio over the entire waveguide band was measured using a slotted line and a well matched sliding load in the reduced height guide.[3] A comparison of the measured and computed VSWR for each of the transformers appears in Fig. 4. Calculated values of the normalized cutoff wavenumber $k_c/k_{c_0}(k_{c_0}=2\pi/4a)$ versus position along the length of the taper are shown in Fig. 5 for the three transformer ratios. Notice that the cutoff frequency in the full- to one-quarter-height transition increases to 1.35 times its value in rectangular waveguide ($s/a=1$). This effect reduces the usefulness of the transformer near the low end of the waveguide band. Two simple remedies to this problem are given in Section VI.

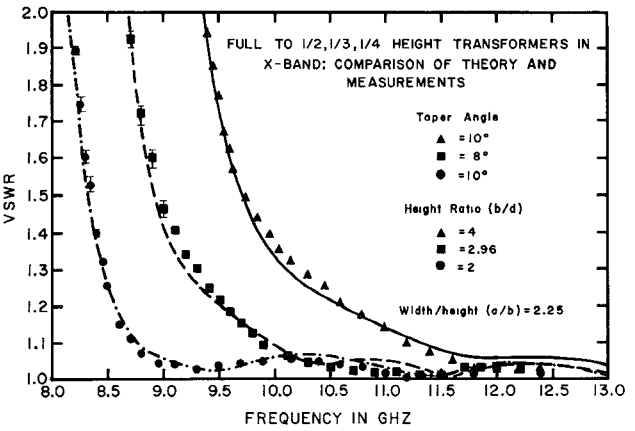

Fig. 4. Comparison of measured and predicted VSWR for three X-band transformers with linear tapers. The lines are the computed values; points, the measured values. Error bars reflect the mismatch uncertainties of the sliding load.

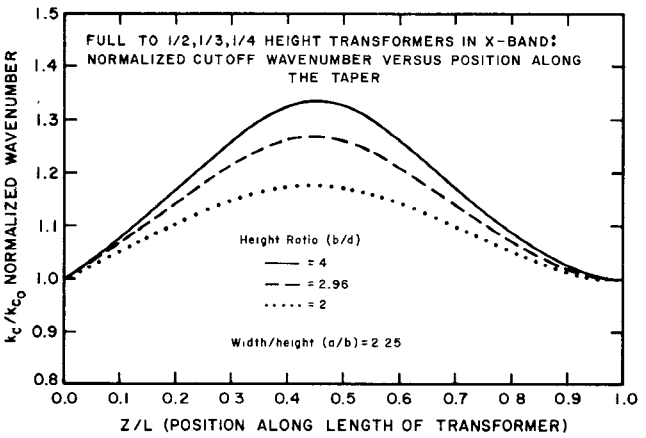

Fig. 5. Predicted values of the normalized cutoff wavenumber versus position along the taper for the transformers of Fig. 4. The cutoff wavenumber of the channel waveguide k_c is normalized to that of standard X-band waveguide $k_{c_0}=2\pi/4a$, where a is the waveguide half-width.

The agreement between the theory and the experimental data is fairly good except at very low values of VSWR. This discrepancy cannot be accounted for by measurement errors and is especially noticeable in the full- to one-quarter-height design. As can be seen in Fig. 6, the only higher order TE mode able to propagate in any portion of the transition is the TE_{20} mode which, being asymmetrical, should not be excited in this structure. Although the magnitude of the reflection coefficient is particularly sensitive to the value of k_c, an error in this variable would show up at all frequencies and not simply when the VSWR is low. The calculation of C_d, the discontinuity capacitance associated with the edge of the channel (see Appendix A), takes into account proximity effects when the channel width is small but not when it approaches the outer dimensions of

[2]One other approach brought to the authors' attention by one of the reviewers is the WKB method discussed by Leonard and Yen [19] in their analysis of flared waveguide junctions. We have not attempted to evaluate this method.

[3]The load was fabricated from LDV Radite #75 tapered to a single point at the side wall of the reduced height waveguide.

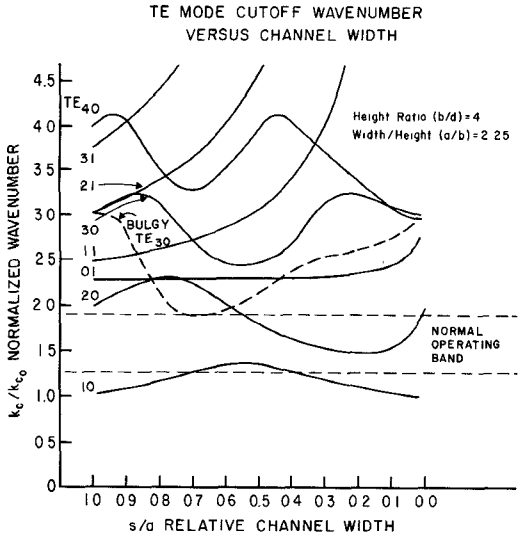

Fig. 6. The TE-mode wavenumbers, normalized to those of *X*-band rectangular waveguide, along the length of the full- to one-quarter-height transformer of Fig. 4. The normal operating band is bounded by the horizontal broken lines. The broken curve represents the TE_{30} mode of a *bulgy* transformer, discussed in Section VI.

the guide ($s \approx a$). It was found that an increase in the value of C_d in the region where s is close to a will have a noticeable effect on the VSWR wherever the reflection coefficient is small. The effect is to bring the measured and predicted performance into closer agreement.

Because of the observed discrepancies between the theory and measurements for small values of VSWR, the design curves given in the next section must be used with a degree of caution. Clearly, if one does not deviate significantly from the three prototypes in this section the theory will adequately predict the transformer performance. For transformer ratios and taper angles which are substantially different, the design curves in Section V should not be relied on to give precise VSWR values below 1.1. For general use, however, the curves should enable the designer to select an easily fabricated transformer to meet his needs.

V. Design Curves

The algorithm described in Section III and Appendix A was used to analyze two different types of channel waveguide transformer. Those of the first type have circular-arc-shaped tapers which could be produced with slitting saws of various diameters, while those of the second type have linear tapers with various half angles. The former design is somewhat easier to fabricate at millimeter wavelengths, whereas the latter configuration is more suitable for use at lower frequencies where the required slitting saw diameters would be prohibitively large. Transformers with input to output height ratios of 2, 3, and 4 were examined. In every case the taper was divided into 50 cross sections for the analysis. Increasing this number had no significant effect on the results.

Plots of the predicted VSWR versus normalized frequency for the transformers with the circular-arc-shaped tapers are shown in Figs. 7–9. The three curves represent transformers whose lengths are 1.5, 2, and 2.5 times the guide wavelength in standard rectangular waveguide at the

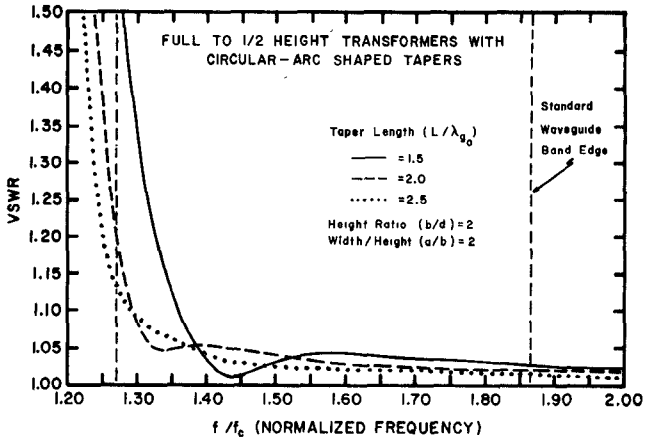

Fig. 7. Predicted VSWR versus normalized frequency for three full- to one-half-height transformers with circular-arc-shaped tapers. The curves represent transformers whose lengths are 1.5, 2, and 2.5 times the guide wavelength in rectangular waveguide at the center of the band ($\lambda_{g_0} = 4a/(1-(f_c/f_0)^2)^{1/2}$, with $f_0/f_c = 1.57$). The frequency is normalized to the cutoff frequency of the rectangular waveguide $f_c = c/4a$. The slitting saw radius used to produce a particular taper is given by $R/a = 13.461(L/\lambda_{g_0})^2 + 0.5$. The width to height ratio (a/b) of the full-height waveguide is 2:1, which is characteristic of most millimeter waveguides. The two vertical lines indicate the normal operating band.

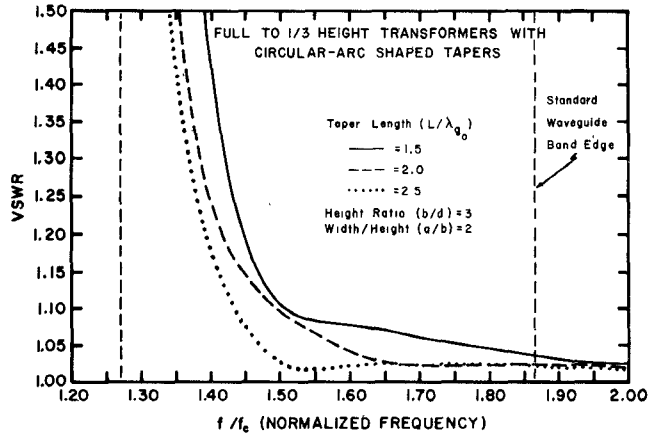

Fig. 8. Predicted VSWR versus normalized frequency for three full- to one-third-height transformers with circular-arc-shaped tapers. The transformers have the same lengths and width-to-height ratio as in Fig. 7.

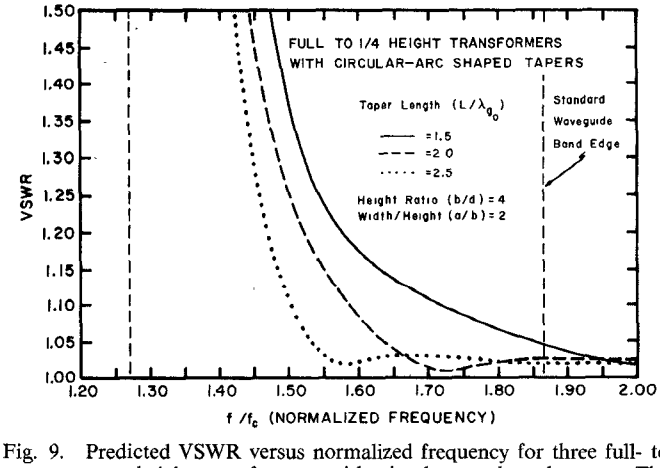

Fig. 9. Predicted VSWR versus normalized frequency for three full- to one-quarter-height transformers with circular-arc-shaped tapers. The same conditions apply as in Fig. 7 and Fig. 8.

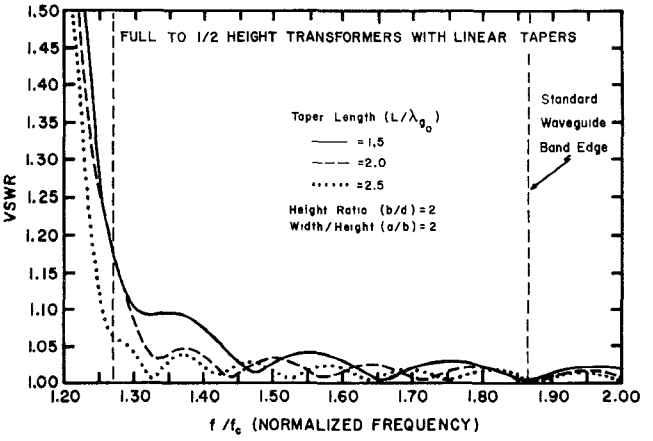

Fig. 10. Predicted VSWR versus normalized frequency for three full- to one-half-height transformers with linear tapers. The curves represent tapers with half-angles chosen to give the same overall length as those of Figs. 7–9, i.e., $\theta = \arctan(0.1927/(L/\lambda_{g_0}))$. All other conditions are the same as in Figs. 7–9.

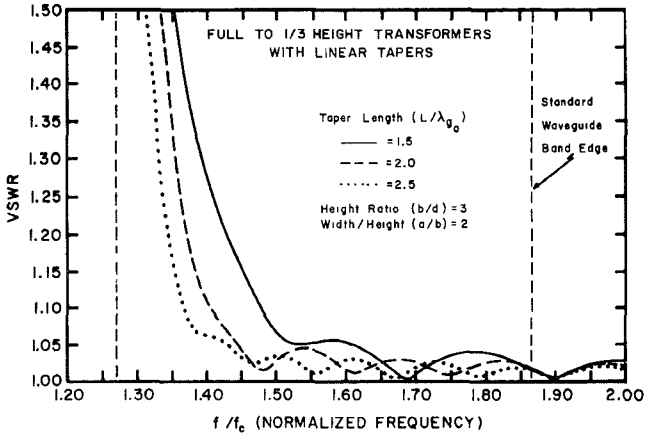

Fig. 11. Predicted VSWR versus normalized frequency for three full- to one-third-height transformers with linear tapers. The taper half-angles are chosen to give transition lengths identical to those of Figs. 7–10. All other conditions are the same as in Figs. 7–10.

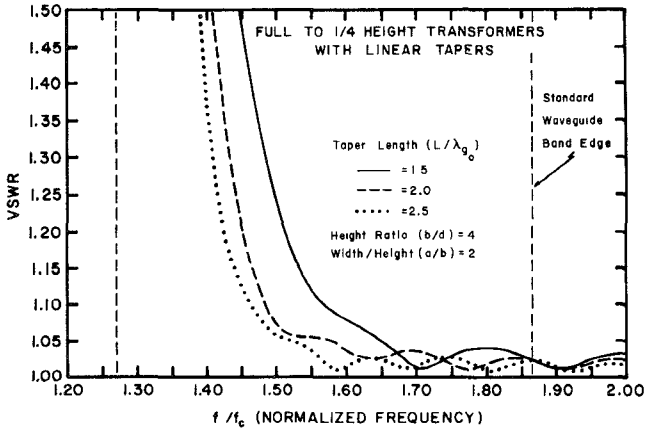

Fig. 12 Predicted VSWR versus normalized frequency for three full- to one-quarter-height transformers with linear tapers. All other conditions are identical to those of Figs. 10 and 11.

center of the band. The design data for transformers with linear tapers are given in Figs. 10–12, where the predicted VSWR for transitions with different half-angles are shown. The half-angles are chosen to yield taper lengths equal to

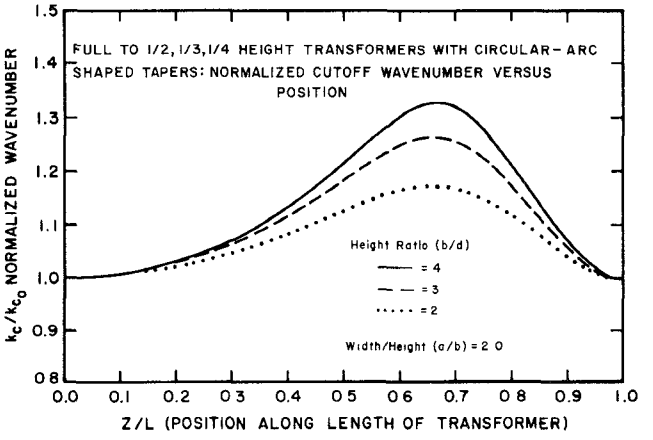

Fig. 13. Predicted values of the normalized wavenumber versus position along the transition for the three circular-arc-shaped transformers in Figs. 7–9. The wavenumber is normalized to that in the rectangular waveguide at the start of the taper ($k_{c_0} = 2\pi/4a$), and the ratio of guide width to full height is assumed to be 2:1, characteristic of standard millimeter waveguides.

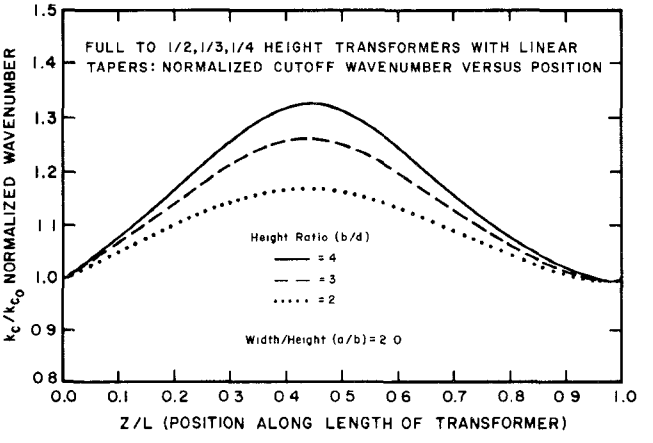

Fig. 14. Predicted values of the normalized wavenumber versus position along the length of the transition for the three linearly tapered transformers of Figs. 10–12. The same conditions apply as in Fig. 13.

those of the circular-arc-shaped transformers in Figs. 7–9. The expected rise in the wavenumber as a function of position along the taper is plotted in Figs. 13 and 14 for both sets of transformers.

The overall performance of the transformers with linear tapered transitions is slightly better than those with circular-arc-shaped profiles. Transformers of large input to output height ratios do not perform well at the low end of their waveguide bands regardless of their length. Fairly good performance can be expected, however, if one operates far enough above the maximum cutoff frequency in the transition. In the next section, methods of increasing the bandwidth of the transformers are described which lead to designs having useful performance over the full waveguide band.

VI. Broad-Band Transformers

Two approaches for improving the low-frequency performance of channel waveguide transformers were investigated. The first is to use two transformers with low height ratios in series to achieve the desired overall ratio. It is

clear from Figs. 13 and 14 that the cutoff frequency of a channel waveguide transformer is related to the input and output waveguide heights. Two transformers of low height ratio in series should have a lower VSWR than a single high-ratio transition.

A second way of improving the low-frequency performance is to vary the waveguide width along the transformer, which can be done without significantly complicating the fabrication procedure. This approach is suggested by the observation, based on Figs. 13 and 14, that the cutoff frequency of a channel waveguide transformer is governed by the dimensions of the cross section with the highest value of k_c/k_{c_0}, which occurs when $s/a \approx 0.55$.

A. Two-Stage Transformers

The analysis of a transformer from full- to half-height in series with a half- to quarter-height transformer indicates a substantial improvement in performance across the waveguide band. The maximum cutoff frequency in the transition is reduced to that of the full- to half-height transformer design. Measurements on a transformer of this type in WR-10 (75–110 GHz) waveguide confirmed the theoretical results.

The approach could be extended to produce a transformer with many steps in height. If the individual tapers were to overlap, the resulting structure could be analyzed using the same method as in Appendix A. No design curves are offered here because of the large number of free parameters.

B. Bulgy Transformers

To make a channel waveguide transformer with increased width near the middle of its length, the same setup and cutting tool can be used as for the unmodified design. Upon completing the reduced height waveguide section (as in Fig. 1(a)) one simply moves the slitting saw to the center of what is to be the transition region, and plunges downwards, producing a circular-arc-shaped bulge in the narrow wall of the guide. The length of the bulge is determined by the slitting saw radius R and the depth of the cut according to $L_B = (2hR - h^2)^{1/2}$ where h is the depth at the midpoint of the bulge.

Figs. 15 and 16 show the results of the theoretical analysis on a group of full- to one-quarter-height bulgy channel waveguide transformers in which the bulges extend the full length of the transition. The transformer lengths correspond to those of Figs. 7–12 and the bulge depths, fixed by the slitting saw radii, increase the reduced height waveguide width by ~ 25 percent at the midpoint of the transition.

Figs. 17 and 18 show the normalized wavenumber along the longitudinal axis of the transformers. The maxima have been reduced significantly compared with the corresponding bulgeless transformers of Figs. 13 and 14. The analysis indicates that transformers with circular-arc-shaped tapers will perform better than those with linear tapers when a bulge is added to the width of the reduced height section. Using this design, it is possible to reduce the VSWR to less than 1.2 over the full waveguide band.

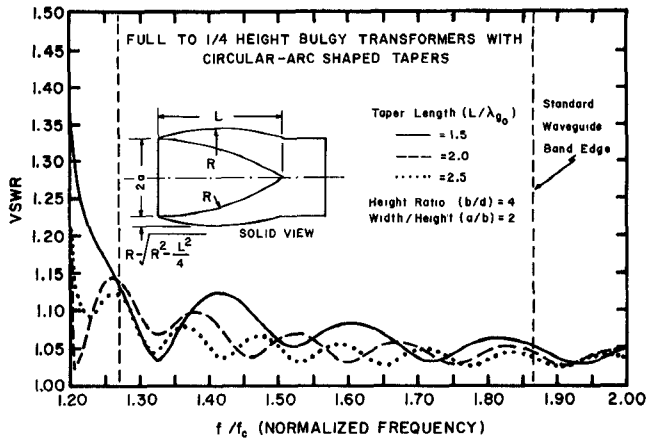

Fig. 15. Predicted VSWR versus normalized frequency for three full- to one-quarter-height bulgy transformers with circular-arc-shaped tapers. Each curve corresponds to one of the transformers in Fig. 9, modified with a bulge in the width of the reduced height waveguide. The bulges are made with the same slitting saw used to produce the rest of the transformer and extend the full length of the transition. The reduced height waveguide width is increased by a maximum of ~ 25 percent at the midpoint of the taper.

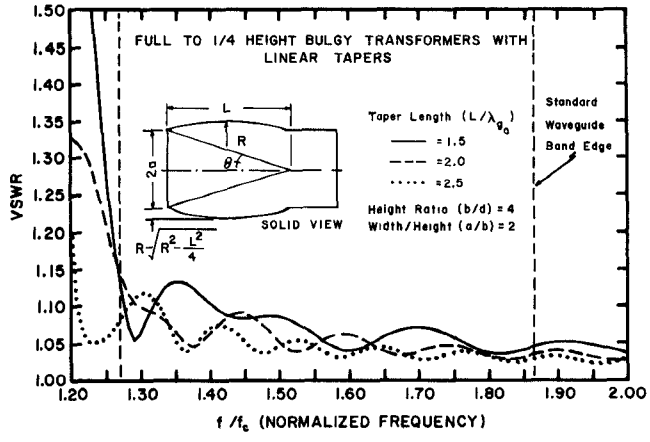

Fig. 16. Predicted VSWR versus normalized frequency for three full- to one-quarter-height bulgy transformers with linear tapers. Each curve corresponds to one of those in Fig. 12. All other conditions are the same as in Fig. 15.

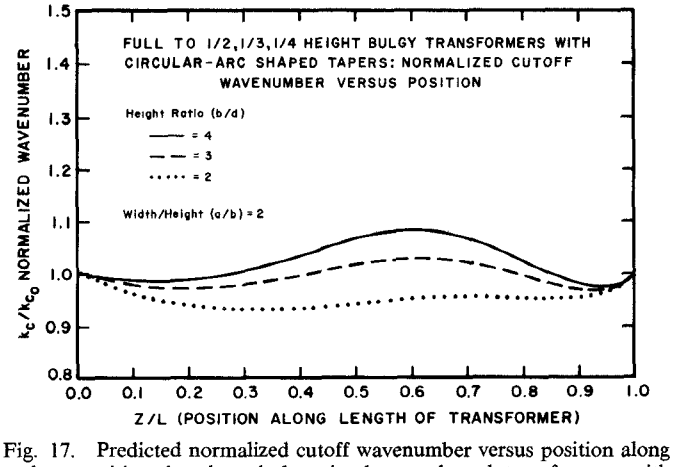

Fig. 17. Predicted normalized cutoff wavenumber versus position along the transition for three bulgy circular-arc-shaped transformers with different height ratios. The cutoff wavenumber is normalized to that in the rectangular guide at the start of the taper ($k_{c_0} = 2\pi/4a$) where the width-to-height ratio (a/b) is 2:1. The curves should be compared to the corresponding bulgeless designs of Fig. 13.

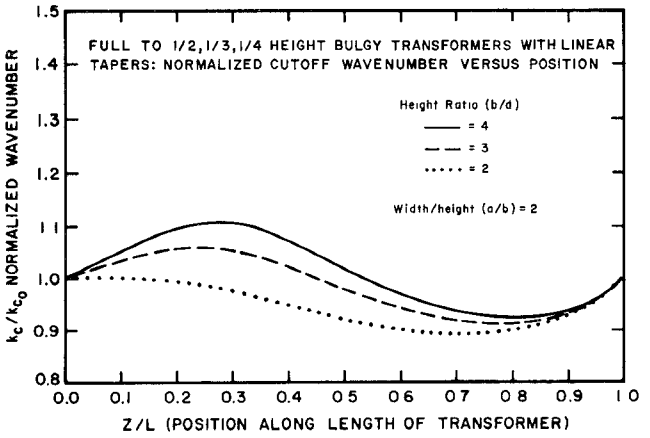

Fig. 18. Predicted values of the normalized cutoff wavenumber versus position along the transition for three linearly tapered, bulgy transformers with different height ratios. The same conditions apply as those of Fig. 17. These curves should be compared to the corresponding bulgeless designs in Fig. 14.

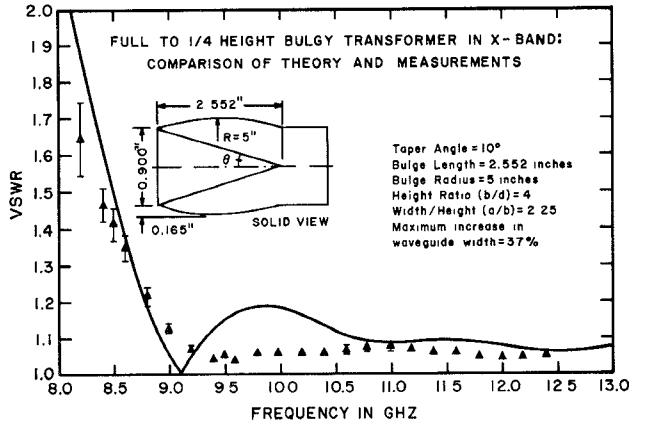

Fig. 19. Measured and predicted VSWR versus frequency for a full- to one-quarter-height bulgy transformer at *X*-band. The transformer is the same as that shown in Fig. 4 with the addition of a bulge in the reduced height waveguide which extends over the full length of the taper. The bulge was made with a rotary milling head, whose effective cutting radius was 5 in, and increases the width of the guide by 37 percent at the midpoint of the transformer. The taper half-angle of the linear transition is 10 degrees, yielding a transformer length of 6.482 cm. Note that at the high-frequency end of the band the TE_{30} mode can propagate in part of this transition (see Fig. 6). The error bars reflect the mismatch uncertainties of the sliding load.

To check the accuracy of the analysis of the bulgy transformer a bulge was made in the full- to one-quarter-height *X*-band channel waveguide transformer described in Section IV. The bulge increased the waveguide width by 37 percent at the maximum and extended over the full length of the taper. The measured and predicted performance are compared in Fig. 19.

The difference between the experimental and theoretical curves here is greater than in the nonbulgy cases. This may be due to the fact that coupling between the fundamental and higher order evanescent modes, especially the TE_{30} mode (see Fig. 6), from one section of the taper to the next, ignored in the analysis, has a greater affect in the bulgy transformers. It is clear, nonetheless, that the addition of a bulge to the transformer results in a significant improvement in low-frequency performance.

VII. Conclusions

A. Summary

A new type of easily fabricated *H*-plane waveguide transformer has been described. The results of a theoretical analysis of the structure agree fairly well with measurements made on *X*-band transformers with input to output height ratios of 2, 3, and 4. Two basic versions of the new design were analyzed and the results presented graphically. The analysis indicates that in its simplest form the transformer is not usable at the lower end of its waveguide band when the height ratio is large. For high-ratio transitions, a two-stage transformer gives better results. The bandwidth of the single-stage transformer can be increased to cover the full waveguide band by increasing the width of the reduced height waveguide in the tapered region. Analysis indicates that the performance of transitions with high impedance ratios could be improved dramatically with only a small increase in waveguide width. Using the same slitting saw to form the reduced height waveguide, the transition section, and the bulge in the width, no additional complication is added to the fabrication process. Measurements of the VSWR of a bulgy full- to one-quarter-height transformer at *X*-band confirmed the predictions of the computer analysis although agreement with theoretical results was not as close as it was for the unmodified transformers.

B. Approximations in the Analysis

The design curves given here should be sufficient in most cases to achieve transformers with a VSWR <1.2 over a full waveguide band. However it is important to ask why the measured and computed results showed consistent discrepancies at low VSWR's, and in the case of the bulgy transformer, why the low-frequency results were not in closer agreement. As mentioned in Section VI-B, the assumption that there is no coupling between the fundamental and higher order evanescent modes in the transition is a possible source of error.

The somewhat arbitrary choice of the voltage and current variables used to define the characteristic impedance of the channel waveguide, discussed in Section III-A, is justified only in that it gives good agreement between theory and experiment. The same definition was used by [7] and [17] in their analyses of ridged waveguides.

The approximations inherent in the transverse resonance and characteristic impedance methods lead to errors whose magnitudes are difficult to estimate. These uncertainties might be circumvented if a finite difference technique [13] for determining the fields in the transformer were combined with the complete mode coupling theory of Solymar [10].

C. Applications

The channel waveguide transformer is particularly suitable for use at millimeter wavelengths where the fabrication of conventional step and tapered transformers is difficult and expensive. The transformer can be formed in a split-block waveguide structure using a single setup on a

milling machine. The block is split in the E-plane which has zero transverse current, and hence poor contact along the joint line will cause no loss.

The authors have successfully used the full- to one-half-height channel waveguide transformer with a circular-arc-shaped taper in two solid-state frequency multipliers, with their outputs in WR-5 and WR-8 waveguide. The equivalent full- to one-quarter-height design has been used in a mixer at 115 GHz. Fabrication time for these devices was reduced dramatically by employing the new transformer. The design is also useful as a transition from the crossed or channel waveguide [1]–[4] to conventional rectangular waveguide.

APPENDIX A
TRANSVERSE RESONANCE SOLUTION FOR $k_{c_{10}}$ AND THE DETERMINATION OF $Z_{c_{10}}$

A. Cutoff Wavenumbers by Transverse Resonance

The method of transverse resonance [14] was applied by Cohn [7] to calculate the TE_{m0}-mode wavenumbers of ridged waveguide. It was later used by Vilmur and Ishii [1] for the determination of the TE_{10}-mode cutoff frequencies of single-channel waveguide. Precisely the same technique can be employed on the double-channel waveguide to obtain the equivalent circuit of Fig. 20 and the following relation involving $k_{c_{10}}$:

$$1-\frac{d}{b}\tan\left(k_{c_{10}}s\right)\tan\left(k_{c_{10}}(a-s)\right) - dk_{c_{10}}\frac{C_d}{\epsilon}\tan\left(k_{c_{10}}(a-s)\right)=0. \tag{A1}$$

This equation has the same form as that derived by Pyle [15] for ridged waveguide when the following identifications are made:

$$Z_1=\left(\frac{\mu}{\epsilon}\right)^{1/2}\frac{b}{l}$$

$$Z_2=\left(\frac{\mu}{\epsilon}\right)^{1/2}\frac{d}{l}$$

$$\alpha=\frac{d}{b}$$

$$\Phi_1=k_{c_{10}}s$$

$$\Phi_2=k_{c_{10}}(a-s)$$

$$B=\frac{k_{c_{10}}C_d l}{(\mu\epsilon)^{1/2}}. \tag{A2}$$

C_d is a discontinuity capacitance which accounts for the generation of higher order modes at the edge of the channel. Whinnery and Jamieson [16] approximated C_d to a high degree of accuracy by

$$\frac{C_d}{\epsilon}=G\cdot\frac{1}{\pi}\left[\frac{\alpha^2+1}{\alpha}\cosh^{-1}\left(\frac{1+\alpha^2}{1-\alpha^2}\right)-2\ln\left(\frac{4\alpha}{1-\alpha^2}\right)\right]. \tag{A3}$$

The multiplier G is a proximity effect term which decreases the value of C_d when the channel width becomes small ($s/a\approx 0$) and the discontinuities can no longer be considered as being isolated from one another. It is given, for two values of α, by Whinnery and Jamieson [16, fig. 15]. When the channel height $2b$ approaches a half wavelength, the value of C_d must be increased. The effect is small, <10 percent for operation in the standard waveguide band, but can be incorporated into (A3) by multiplying C_d by a correction factor given in Whinnery and Jamieson [16, Fig. 16].

A computer program was written to solve the transcendental equation (A1) iteratively for the lowest order root. The resulting values of $k_{c_{10}}$ for 10 positions along the length of a full- to one-quarter-height transformer in X-band waveguide are listed in Table I.

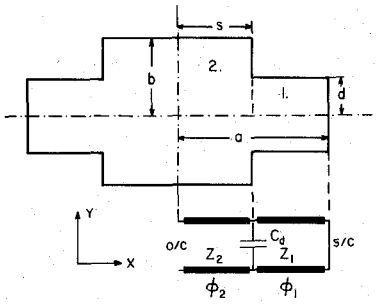

Fig. 20. A cross-sectional view of the channel waveguide with the equivalent circuit used to derive the wavenumbers by the transverse resonance method of Appendix A. For the wave equation solutions described in Appendix B, the cross section is divided into the two regions indicated in the figure and the fields in each are expanded as series of orthogonal functions. The final solutions are determined after the application of the boundary conditions, which require matching of the tangential fields at the line dividing regions 1 and 2.

TABLE I
COMPARISON OF METHODS USED IN APPENDICES A AND B ON THE FULL- TO ONE-QUARTER-HEIGHT TRANSFORMER OF FIG. 4

Normalized Channel Width (s/a)	Position Along Taper in cm. (z)	Cutoff Wavenumber by Transverse Resonance (k_c)	Cutoff Wavenumber by 3x3 Matrix Solution (k_c)	Cutoff Wavenumber by 7x7 Matrix Solution (k_c)	Impedance by TEM Approx.-App. A (Z_c/Z_w)	Impedance by Field Solutions from App. B (Z_c/Z_w)
1.0	0.0000	1.3743	1.3743	1.3743	0.6981	0.6981
0.9	0.6482	1.4845	1.4845	1.4845	0.7360	0.7313
0.8	1.2965	1.6073	1.6075	1.6073	0.7446	0.7310
0.7	1.9447	1.7323	1.7330	1.7321	0.6982	0.6766
0.6	2.5929	1.8248	1.8268	1.8240	0.5702	0.5581
0.5	3.2411	1.8275	1.8507	1.8261	0.4273	0.4057
0.4	3.8894	1.7380	1.7430	1.7375	0.3136	0.2975
0.3	4.5376	1.6137	1.6210	1.6157	0.2473	0.2355
0.2	5.1858	1.4972	1.5050	1.5002	0.2096	0.2009
0.1	5.8340	1.4107	1.4162	1.4122	0.1876	0.1822

B. Characteristic Impedance

As discussed in Section III-A, the characteristic impedance in the channel waveguide is not unique. Cohn [7] and Mihran [17] defined a characteristic impedance in ridged waveguide using the transverse voltage at the center of the guide divided by the total longitudinal current on the top face. We have found that this definition, when applied to the channel waveguide transformer, gives acceptable agreement with experiment.

In a manner analogous to that of Mihran [17] we obtain for the channel waveguide

$$Z_{c_{1V}}=\frac{Z_w}{\frac{C_d}{\epsilon}\cos\left(k_{c_{10}}s\right)+\frac{1}{bk_{c_{10}}}\left[\sin\left(k_{c_{10}}s\right)+\frac{b}{d}\cos\left(k_{c_{10}}s\right)\tan\left(\frac{k_{c_{10}}}{2}(a-s)\right)\right]} \tag{A4}$$

where

$$Z_w = \frac{\omega\mu}{\beta} = \frac{\left(\frac{\mu}{\epsilon}\right)^{1/2}}{\left[1-\left(\frac{f_c}{f}\right)^2\right]^{1/2}} \tag{A5}$$

is the TE-mode wave impedance. The equation has the same form as Mihran's equation (2). Note that C_d contains a frequency dependent term which should be included in the solution of (A4).

Appendix B
Wave Equation Solution for $k_{c_{10}}$ and the Determination of $Z_{c_{10}}$

A. Cutoff Wavenumbers from the Wave Equation

The field relations derived by Tham [3] for the channel waveguide are given in (A6)–(A14). The unnormalized expressions for the TE_{10} magnetic fields at any cross section along the length of the channel waveguide transformer are (referring to Fig. 20)

$$H_{z_1} = \sum_{r=0,2,4,\cdots}^{\infty} \Phi_{1_r} \cosh\left(p_{1_r}\left(\frac{x}{2a}-\frac{1}{2}\right)\right)\cos\left[\frac{r\pi}{2d}(d-y)\right] \tag{A6}$$

and

$$H_{z_2} = \sum_{m=0,2,4,\cdots}^{\infty} \Phi_{2_m} \sinh\left(p_{2_m}\frac{x}{2a}\right)\cos\left(\frac{m\pi}{2b}(b-y)\right) \tag{A7}$$

where Φ_{1_r} and Φ_{2_m} are complex constants. Also

$$p_{1_r}^2 = -4k_{c_{10}}^2 a^2 + \left(\frac{r\pi a}{d}\right)^2 \tag{A8}$$

and

$$p_{2_m}^2 = -4k_{c_{10}}^2 a^2 + \left(\frac{m\pi a}{b}\right)^2. \tag{A9}$$

Subscript 1 refers to the region $s \leqslant x \leqslant a$, $0 \leqslant y \leqslant d$ and subscript 2 refers to the region $0 \leqslant x \leqslant s, 0 \leqslant y \leqslant b$. The eigenvalue equation which must be solved to find the wavenumbers $k_{c_{10}}$ is

$$\sum_{n=0,2,4,\cdots}^{\infty} \sum_{m=0,2,4\cdots}^{\infty} \Phi_{2_m} a_{nm} = 0. \tag{A10}$$

This has a solution if

$$\det[\boldsymbol{a}] = 0. \tag{A11}$$

a_{nm} is given by

$$a_{nm} = \sinh\left(p_{2_m}\frac{s}{2a}\right) \cdot \left[\left\{\frac{4d}{b}\sum_{r=0,2,4,\cdots}^{\infty} p_{1_r}\frac{C_{rn}C_{rm}}{\Delta_r}\tanh\left(p_{1_r}\left(\frac{s}{2a}-\frac{1}{2}\right)\right)\right\} - \frac{p_{2_m}\Delta_m\delta_{nm}}{\tanh\left(p_{2_m}\frac{s}{2a}\right)}\right] \tag{A12}$$

where

$$C_{mn} = \frac{1}{d}\int_0^d \cos\left(\frac{m\pi}{2d}(d-y)\right)\cos\left(\frac{n\pi}{2b}(b-y)\right)dy. \tag{A13}$$

Φ_{1_m} and Φ_{2_m} are related by

$$\Phi_{1_m} = \frac{2}{\Delta_m \cosh\left(p_{1_m}\left(\frac{s}{2a}-\frac{1}{2}\right)\right)} \sum_{n=0,2,4,\cdots}^{\infty} \Phi_{2_n} C_{mn} \sinh\left(p_{2_n}\frac{s}{2a}\right) \tag{A14}$$

where

$$\Delta_m = 2 \text{ if } m = 0$$
$$= 1 \text{ otherwise.}$$

A computer program was written to solve (A6)–(A14) for $k_{c_{10}}$ and $H_{z_{10}}$. It was found that the infinite sums could be truncated to the first three terms without appreciable loss of accuracy. The solutions to (A11) provide all the $TE_{odd,even}$-mode wavenumbers, but only the lowest nonzero value is required for calculating $k_{c_{10}}$. An initial guess for $k_{c_{10}}$ is taken to be the TE_{10} rectangular guide wavenumber; (A8), (A9), and (A13) are calculated; the matrix terms in (A12) are formed; and (A11) is solved using the IBM SSP program MINV. There is no effect on the solution of (A11) if a_{nm} in (A12) is divided through by the sinh term outside the brackets. The terms in the matrix will then all be real, since p_1 and p_2 are always pure real or pure imaginary, and the evaluation of the determinant is considerably faster. If the solution of (A11) is greater than a specified limit, then $k_{c_{10}}$ is incremented, $\boldsymbol{a}$ is reformed, and the determinant reevaluated. Following the suggestion in [4], if a sign change occurs in the value of the determinant, then the increment for $k_{c_{10}}$ is halved and its sign is reversed. Usually $k_{c_{10}}$ converges to 8 decimal places within 40 iterations when a 3×3 matrix is used. When more than five terms are used in the series in (A6)–(A14) the solution of (A11) becomes a very sensitive function of $k_{c_{10}}$ and the eigenvectors in (A10) are then difficult to determine accurately. In Table I, the values of $k_{c_{10}}$ as found from (A11) are compared with those obtained from the solution by the transverse resonance method ((A1)) for ten values of the channel width. Results are shown with the series truncated at 3 and 7 terms. The two methods agree to within 0.5 percent.

Once the values of $k_{c_{10}}$ at each cross section have been determined, they are used in (A10) to find the values of the TE_{10}-mode eigenvectors. The IBM SSP program MFGR can be used for this purpose since $\boldsymbol{a}$ is now a real matrix. The rank of $\boldsymbol{a}$ is always the number of rows -1, and therefore the eigenvectors for the terms $n > 0$ are expressed as multiples of the $n = 0$ term. This causes no difficulty in determining the characteristic impedance since the arbitrary constant divides out. The sinh factor taken out of (A12) must now be replaced to obtain the desired

eigenvectors. If required, a value for the arbitrary constant can be established by normalizing the transverse fields in some way, usually so that the power flow at each cross section is unity. When the Φ_{2_m}'s have been determined, the Φ_{1_r}'s can be found from (A14). Substitution into (A6)–(A7) then gives the expressions for the longitudinal field components in the two regions of the channel waveguide cross section. Similar expressions can be obtained using the Ritz-Galerkin method as in [4] or by breaking the cross section along the $y = d$ line rather than along $x = s$.

B. Characteristic Impedance

The characteristic impedance is derived from the equivalent voltage and current as discussed in Appendix A. The maximum transverse voltage at the center of the channel is determined by integrating the electric field, $E_y \propto \partial H_z/\partial x$, from $-b$ to b (by symmetry $E_x = 0$ along this line). The total longitudinal current along the upper half ($y > 0$) of the channel waveguide is then found by integrating the transverse magnetic field along the walls, and Z_c is calculated by dividing V by I.

The steps leading to the calculation of Z_c are as follows:

$$Z_c = V/I \tag{A15}$$

with

$$V = -\int \boldsymbol{E}_t \cdot d\boldsymbol{l}_1 = \text{transverse voltage} \tag{A16}$$

and

$$I = \int \boldsymbol{H}_t \cdot d\boldsymbol{l}_2 = \text{longitudinal current.} \tag{A17}$$

$\boldsymbol{E}_t$ and $\boldsymbol{H}_t$ are transverse field vectors in the waveguide. They are related to the TE_{10} orthogonal mode vector functions by

$$\boldsymbol{E}_t \equiv V_{10}\boldsymbol{e}_{10} \tag{A18}$$

$$\boldsymbol{H}_t \equiv I_{10}\boldsymbol{h}_{10} \tag{A19}$$

where $\boldsymbol{e}_{10}$ and $\boldsymbol{h}_{10}$ are derived from the transverse scalar wave equation

$$\nabla_t^2 \Psi_{10} + k_{c_{10}}^2 \Psi_{10} = 0 \tag{A20}$$

using

$$\boldsymbol{e}_{10} = \hat{\boldsymbol{z}} \times \nabla_t \Psi_{10} \tag{A21}$$

and

$$\boldsymbol{h}_{10} = \hat{\boldsymbol{z}} \times \boldsymbol{e}_{10} \tag{A22}$$

with

$$\int\int \boldsymbol{e}_{10} \cdot \boldsymbol{e}_{10}^* \, d\boldsymbol{A} = 1. \tag{A23}$$

The longitudinal fields in (A6) and (A7) are related to Ψ_{10} by

$$H_z = \frac{V_{10} k_{c_{10}}^2 \Psi_{10}}{jk_0 \left(\frac{\mu}{\epsilon}\right)^{1/2}} \tag{A24}$$

where $k_{c_{10}}$ is the wavenumber in the guide at cutoff and k_0 is the wavenumber in free-space.

The transverse fields in (A18) and (A19) can be expressed in terms of H_z using Maxwell's equations

$$\boldsymbol{E}_t = V_{10}\boldsymbol{e}_{10} = V_{10}\left(e_{10_x}\hat{\boldsymbol{x}} + e_{10_y}\hat{\boldsymbol{y}}\right) = \frac{-jk_0^2}{k_{c_{10}}^2}\left(\frac{\mu}{\epsilon}\right)^{1/2}\left(\frac{\partial H_z}{\partial y}\hat{\boldsymbol{x}} - \frac{\partial H_z}{\partial x}\hat{\boldsymbol{y}}\right) \tag{A25}$$

$$\boldsymbol{H}_t = I_{10}\boldsymbol{h}_{10} = I_{10}\left(-e_{10_y}\hat{\boldsymbol{x}} + e_{10_x}\hat{\boldsymbol{y}}\right) = \frac{-jk_0}{k_{c_{10}}^2}\left(\frac{\mu}{\epsilon}\right)^{1/2}\frac{I_{10}}{V_{10}}\left(\frac{\partial H_z}{\partial x}\hat{\boldsymbol{x}} + \frac{\partial H_z}{\partial y}\hat{\boldsymbol{y}}\right). \tag{A26}$$

The transverse voltage at the center of the channel waveguide is found from

$$V = -2\int_0^b \boldsymbol{E}_{t_2}\, dy = \frac{-j2k_0\left(\frac{\mu}{\epsilon}\right)^{1/2}}{k_{c_{10}}^2}\int_0^b \left(\frac{\partial H_{z_2}}{\partial x}\right) dy \tag{A27}$$

where H_{z_2} is obtained from (A6).

The total longitudinal current along the upper half of the channel waveguide is given by

$$I = 2\left[\int_0^s \boldsymbol{H}_{t_2}\, dx + \int_s^a \boldsymbol{H}_{t_1}\, dx + \int_d^b \boldsymbol{H}_{t_2}\, dy + \int_0^d \boldsymbol{H}_{t_1}\, dy\right] \tag{A28}$$

$$- \frac{j2k_0}{k_{c_{10}}^2}\left(\frac{\mu}{\epsilon}\right)^{1/2}\frac{I_{10}}{V_{10}}\left[\int_0^s \left(\frac{\partial H_{z_2}}{\partial y}\right) dx + \int_s^a \left(\frac{\partial H_{z_1}}{\partial y}\right) dx + \int_d^b \left(\frac{\partial H_{z_2}}{\partial x}\right) dy + \int_0^d \left(\frac{\partial H_{z_1}}{\partial x}\right) dy\right]. \tag{A29}$$

Substituting for H_{z_1} and H_{z_2} from (A6) and (A7) and carrying out the integrations we obtain

$$Z_c = \frac{V}{I} = \frac{Z_w \Phi_{2_0} p_{2_0} \frac{b}{a}}{\sum_{m=0,2,4,\cdots}^{\infty} \left\{ \Phi_{2_m} \sinh\left(p_{2_m}\frac{s}{2a}\right) + \Phi_{1_m}\left[1 - \cosh\left(p_{1_m}\left(\frac{s}{2a} - \frac{1}{2}\right)\right)\right] - \Phi_{2_m}\sinh\left(p_{2_m}\frac{s}{2a}\right)\left[1 - \cos\left(\frac{m\pi}{2b}(b-d)\right)\right] + \Phi_{1_m}\left(1 - \cos\left(\frac{m\pi}{2}\right)\right)\right\}} \tag{A30}$$

where $Z_w = V_{10}/I_{10} = \omega\mu/\beta$ is the wave impedance for TE modes. Z_c is real and positive above cutoff.

In Table I, the value of Z_c at infinite frequency (before multiplying through by Z_w), as determined from (A30), is compared with the value obtained from (A4). The results agree to within ~ 5.0 percent.

As discussed in Section III-B, the field expressions in (A6)–(A7) converge very slowly in the region near the start of the channel. If we plot the x and y components of the

transverse electric field along the line $x = s$, we see (Fig. 3) that the truncated series expressions are a poor approximation to the actual fields. The tangential fields in regions 1 and 2 of Fig. 2 should be identical along the line $y = 0$ to d, and for larger y values E_y in region 2 must go to zero. At the corner $x = s$, $y = d$, both field components should become infinite.

Fortunately, the determination of the characteristic impedance is most strongly dependent on the fields along $y = d$ and $y = b$ and is not affected greatly by the integral along the side wall of the channel. The same statement cannot be made for the calculation of the terms in the mode coupling theory discussed in Section III-B.

Acknowledgment

The authors would like to thank Dr. L. Solymar for some useful references, Dr. P. J. Khan for his helpful discussion, and E. Michaud for her preparation of the manuscript.

References

[1] R. J. Vilmur and K. Ishii, "The channel waveguide," *IRE Trans. Microwave Theory Tech.*, vol. MTT-10, pp. 220–221, May 1962.
[2] N. A. Kuz'min and T. V. Makarov, "Electromagnetic waves in a rectangular cross-shaped waveguide," *Radio Eng. Electron. Phys.*, vol. 6, pp. 1781–89, Dec. 1961.
[3] Q. C. Tham, "Modes and cutoff frequencies of crossed rectangular waveguides," *IEEE Trans. Microwave Theory Tech.*, vol. MTT-25, pp. 585–588, July 1977.
[4] F. L. C. Lin, "Modal characteristics of crossed rectangular waveguides," *IEEE Trans. Microwave Theory Tech.*, vol. MTT-25, pp. 756–763, Sept. 1977.
[5] R. C. Johnson, "Design of linear double tapers in rectangular waveguides," *IRE Trans. Microwave Theory Tech.*, vol. MTT-7, pp. 374–378, July 1959.
[6] S. A. Schelkunoff, "Impedance concept in wave guides," *Quart. J. Appl. Math.*, vol. II, no. 1, pp. 1–15, Apr. 1944.
[7] S. B. Cohn, "Properties of ridge waveguide," *Proc. IRE*, vol. 35, pp. 783–788, Aug. 1947.
[8] S. A. Schelkunoff, "Conversion of Maxwell's equations into generalized Telegraphist's equations," *Bell Syst. Tech. J.*, vol. 34, pp. 995–1043, Sept. 1955.
[9] G. Reiter, "Generalized Telegraphist's equation for waveguides of varying cross section," *Proc. Inst. Elec. Eng.*, Part B, vol. 106, Sup. no. 13, pp. 54–57, Sept. 1959.
[10] L. Solymar, "Spurious mode generation in nonuniform waveguide," *IRE Trans. Microwave Theory Tech.*, vol. MTT-7, pp. 379–383, July 1959.
[11] B. Z. Katzenelenbaum, "On the theory of nonuniform waveguides with slowly changing parameters," presented at Congr. Int. Circuits Antennes Hyperfréquences; also in *Suppl. Onde Elec.*, no. 376, pp. 124–127, Aug. 1958.
[12] J. P. Montgomery, "On the complete eigenvalue solution of ridged waveguide," *IEEE Trans. Microwave Theory Tech.*, MTT-19, pp. 547–555, June 1971.
[13] S. S. Saad, J. B. Davies, and O. J. Davies, "Computer analysis of gradually tapered waveguide with arbitrary cross sections," *IEEE Trans. Microwave Theory Tech.*, MTT-25, pp. 437–440, May 1977.
[14] S. Ramo and J. R. Whinnery, *Fields and Waves in Modern Radio*. New York, NY: Wiley, 1944.
[15] J. R. Pyle, "The cutoff wavelength of the TE_{10} mode in ridged rectangular waveguide of any aspect ratio," *IEEE Trans. Microwave Theory Tech.*, MTT-14, pp. 175–183, Apr. 1966.
[16] J. R. Whinnery and H. W. Jamieson, "Equivalent circuits for discontinuities in transmission lines," *Proc. IRE*, vol. 32, pp. 98–114, Feb. 1944.
[17] T. G. Mihran, "Closed- and open-ridge waveguide," *Proc. IRE*, vol. 37, pp. 640–644, June 1949.
[18] F. Sporleder and H. G. Unger, *Waveguide Tapers Transitions and Couplers*. Stevenage, U.K.: Peter Peregrinus, Ltd., 1979.
[19] D. J. Leonard and J. L. Yen, "Junction of smooth flared wave guides," *J. Appl. Phys.*, vol. 28, no. 12, pp. 1441–1448, Dec. 1957.

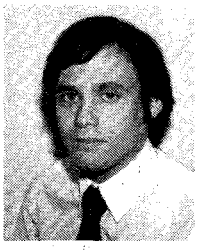

Peter H. Siegel (S'78) was born in New Rochelle, NY, in 1954. He received the B.A. degree in physics from Colgate University in 1976 and an M.S. in electrical engineering from Columbia University in 1978. He is currently completing work on his doctoral thesis at Columbia University on the optimization of millimeter-wavelength mixers.

Since 1975 he has been a Research Assistant at the NASA Goddard Institute for Space Studies where he has been doing research on millimeter-wave mixers, frequency multipliers, quasi-optical structures, and waveguide components. His other interests include computer-aided design and submillimeter-wave receivers.

Dorn W. Peterson (M'79) was born in Fargo, ND, in 1947. He received the B.S. degree in physics from Michigan State University in 1969, and the Ph.D. degree from the University of California, Berkeley, in 1978. His thesis was based on experimental and theoretical work concerning Josephson junction parametric amplifiers.

From 1979 to 1981 he was a National Research Council Associate at the Goddard Institute for Space Studies where he worked on quasi-optical mixers and Josephson point contact mixers. Since 1981 he has been with Columbia University where he has been working on Schottky barrier mixers for millimeter-wave receivers.

Anthony R. Kerr (S'64–A'66–SM'78) was born in England on August 30, 1941. He received the B.E., M.Eng.Sc., and Ph.D. degrees from the University of Melbourne, Australia, in 1964, 1967, and 1969, respectively.

In 1969 he joined the Commonwealth Scientific and Industrial Research Organization, Sydney, Australia, to develop low-noise receivers for radio astronomy. From 1971 to 1974 he worked on low-noise cryogenic receivers for millimeter-wave astronomy with the National Radio Astronomy Observatory, Charlottesville, VA. He is now with the NASA/Goddard Institute for Space Studies, New York, NY, developing low-noise receivers for millimeter and submillimeter wavelengths.

Dr. Kerr is a member of URSI Commission J and the Astronomical Society of Australia. He was corecipient of the 1978 Microwave Prize.